

Review Article

# Clinical anatomy of the macula

Seher Koksaldi 1, Mustafa Kayabasi 2, Omer Karti 3 and Ali Osman Saatci 3

- <sup>1</sup> Department of Ophthalmology, Agri Ibrahim Cecen University, Faculty of Medicine, Agri, Turkey
- <sup>2</sup> Department of Ophthalmology, Mus State Hospital, Mus, Turkey
- <sup>3</sup> Department of Ophthalmology, Dokuz Eylul University, Faculty of Medicine, Izmir, Turkey

## **ABSTRACT**

**Background:** The macula is located at the center of the retina and is crucial for high-resolution color vision. Its complex anatomical structure supports a dense array of cone photoreceptors and specialized neuronal pathways essential for central vision. A thorough understanding of macular microanatomy is vital for accurate interpretation of retinal imaging and effective management of macular diseases. This narrative review provides a detailed and integrative overview of macular anatomy, emphasizing clinically relevant microanatomical features and their implications in retinal imaging and macular disease management.

Methods: A PubMed/MEDLINE search was performed using relevant keywords (e.g., "anatomy," "fovea," "foveal avascular zone," "foveola," "Henle fiber layer," "macula," "macular anatomy," "macula lutea," "optical coherence tomography," "parafovea," "perifovea," and "retina") to identify English-language articles published up to February 28, 2025. The reference lists of the included papers were manually reviewed to identify additional relevant sources. The review considered a wide range of study types, including clinical trials, systematic and narrative reviews, meta-analyses, observational studies, case series, and experimental animal studies.

Results: This review highlights the remarkable characteristics of the fovea and foveola, which are densely packed with cone photoreceptors, making them uniquely suited for sharp vision. The surrounding parafoveal and perifoveal regions offer critical structural and functional support, while the Henle fiber layer facilitates the oblique course of photoreceptor axons, further refining central vision. Moreover, high-resolution optical coherence tomography has revolutionized visualization of the macular architecture, enabling a detailed assessment of previously undetectable retinal layers. This review explores key anatomical features, such as the foveal avascular zone, precise photoreceptor organization, and the role of Muller glial cells, in the context of high-resolution imaging. These associations between anatomy and imaging enhance diagnostic precision and may inform targeted treatment approaches for macular diseases.

Conclusions: Comprehensive knowledge of macular anatomy is crucial for the accurate interpretation of retinal imaging and management of central retinal disorders. The bridging of classic histological findings with modern imaging enhances comprehension of the healthy macula and the detection and management of pathological changes. This review serves as a practical anatomical reference for clinicians and researchers in macular diagnostics and therapeutics. Further studies are warranted to explore how emerging imaging technologies can enhance early detection and treatment strategies for macular disorders.

# **KEYWORDS**

anatomies, fovea centralis, foveal avascular zone, foveola, henle fiber layer, macula luteas, optical coherence tomography, parafovea, perifovea, retina

Correspondence: Ali Osman Saatci, Mustafa Kemal Sahil Bulvarı. No: 73, A Blok, Daire: 9, Narlidere, Izmir, Turkey. Email: osman.saatci@gmail.com, ORCID iD: https://orcid.org/0000-0001-6848-7239.

How to cite this article: Koksaldi S, Kayabasi M, Karti O, Saatci AO. Clinical anatomy of the macula. Med Hypothesis Discov Innov Ophthalmol. 2025 Summer; 14(2): 17-27. https://doi.org/10.51329/mehdiophthal1520

Received: 31 May 2025; Accepted: 27 July 2025



Copyright © Author(s). This is an open-access article distributed under the terms of the Creative Commons Attribution-NonCommercial 4.0 International License (https://creativecommons.org/licenses/by-nc/4.0/) which permits copy and redistribute the material just in noncommercial usages, provided the original work is properly cited.

#### **INTRODUCTION**

The macula, situated at the center of the retina, is crucial for achieving the sharpest and most detailed visual perception. Understanding its microanatomy is essential for interpreting high-resolution retinal images and diagnosing macular pathologies [1]. The macula is named for its yellow appearance under red-free illumination, caused by the localized accumulation of xanthophyll pigments—primarily lutein and zeaxanthin—within a circular region approximately 5–6 mm in diameter at the posterior pole of the eye. These pigments are most densely concentrated in the fovea, with levels gradually diminishing toward the periphery [2].

The fovea is a highly specialized macular region that mediates fine vision and color discrimination [3]. It includes the central foveola and surrounding foveal walls, which are inclined. The foveal architecture is defined by unique features, including a capillary- and rod-free zone, high density of cone photoreceptors, and elongated photoreceptor outer segments, all of which contribute to exceptional visual acuity [4]. Foveal pits form through a combination of biomechanical forces and cellular mechanisms, particularly the compactness of cone photoreceptors within this region [5].

The neurosensory retina is a multilayered tissue that lines the inner surface of the eye, adjacent to the vitreous body [6]. It consists of several distinct layers that process and transmit visual information, including the internal limiting membrane, nerve fiber layer, ganglion cell layer, inner and outer plexiform layers, inner and outer nuclear layers, and photoreceptor layer [7]. The outer nuclear layer houses the densely packed nuclei of both rod and cone photoreceptors, which are critical for phototransduction. The outer plexiform layer is crucial in synaptic communication, transmitting signals between photoreceptors and second-order neurons (bipolar and horizontal cells) [8]. The peripheral two-thirds of this layer—the Henle fiber layer—consists of radially oriented photoreceptor axons intermixed with Muller cell processes. The inner third of the layer includes dendritic branches of bipolar and horizontal cells, originating in the inner nuclear layer. A structural distinction between the dendritic and Henle fiber layers lies in their fiber orientations, which may influence the reflective properties observed on optical coherence tomography (OCT) images [9].

OCT has enabled detailed visualization of four reflective layers in the outer retina, ordered from the outermost to the innermost: the retinal pigment epithelium (RPE)–Bruch's membrane complex, the interdigitation zone, the ellipsoid zone, and the external limiting membrane [10]. The RPE is a monolayer of highly polarized cells that are vital for maintaining photoreceptor function. Its physiological roles include clearing photoreceptor outer segment debris, absorbing excess light, dissipating retinal heat, facilitating the visual cycle via vitamin A processing, and supporting the outer blood–retinal barrier and choriocapillaris. The RPE is firmly attached to Bruch's membrane, a five-layered extracellular matrix that serves as a selectively permeable interface between the retina and choroid. Beneath Bruch's membrane lies the choriocapillaris, a capillary network that supplies essential nutrients and oxygen to the outer retina and RPE [11, 12].

This narrative review provides an integrative overview of macular anatomy, highlighting key microstructural elements critical for accurate retinal imaging interpretation and clinical decision making.

## **METHODS**

A literature review was performed using the PubMed/MEDLINE database to identify studies published until February 28, 2025. The targeted search strategy employed a combination of anatomical and imaging-related keywords, including "fovea," "foveola," "macula lutea," "Henle fiber layer," "foveal avascular zone," "parafovea," "perifovea," "macular anatomy," "retina," and "optical coherence tomography." Boolean operators and Medical Subject Headings (MeSH) were applied, where appropriate, to refine the search. Only articles published in English and available in full text were included. Reference lists of the included papers were manually reviewed to identify additional relevant sources. The review considered a wide range of study types, including clinical trials, systematic and narrative reviews, meta-analyses, observational studies, case series, and experimental animal studies.

# **RESULTS and DISCUSSION**

## Anatomy and Histology of the Macula

The macula consists of several clinically significant layers, sublayers, and potential spaces, measuring approximately 6 mm in diameter [3, 8]. It lies in the central retina between the primary retinal vascular arcades, which nourish the inner two-thirds of the retinal layers [3, 8]. The fovea lies at the center of the macula and contains the foveola, a small central pit essential for sharp, detailed vision. The innermost 250–600  $\mu$ m of the macula is devoid of retinal blood vessels and is instead nourished by the choroidal circulation beneath [12].

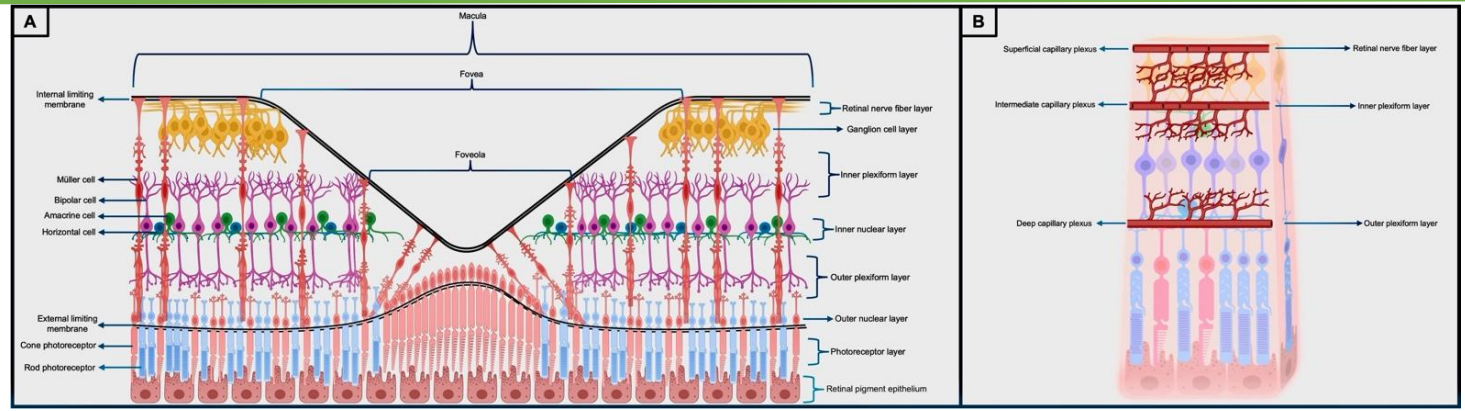


Figure 1. Schematic representation of the structural and vascular organization of the macula. (A) Cross-sectional illustration of the macula demonstrating the specialized laminar arrangement of retinal neurons and glial cells. Key cellular components, including Muller cells, bipolar cells, amacrine cells, horizontal cells, and photoreceptors, are depicted within their respective retinal layers. The fovea and foveola are characterized by thinning of inner retinal layers and dense packing of cone photoreceptors. (B) Schematic demonstrating the laminar distribution of retinal capillary plexuses in relation to the retinal layers. The superficial, intermediate, and deep capillary plexuses are primarily located within the retinal nerve fiber layer, inner plexiform layer, and outer plexiform layer, respectively.

The macular layers, arranged from the innermost to the outermost, include the nerve fiber layer, ganglion cell layer, inner plexiform layer, inner nuclear layer, and outer plexiform layer [13]. Other layers include the outer nuclear layer, outer plexiform layer (also known as the Henle fiber layer), external limiting membrane, and inner segment band (formerly known as the inner segment/outer segment junction). Beyond these are the photoreceptor outer segments and the RPE [14].

In the macular region, the outer plexiform layer (referred to as the Henle fiber layer in the foveal area) contains synapses between photoreceptors and bipolar cells, as well as regulatory input from horizontal cells [13]. In the foveal and parafoveal regions, the outer plexiform layer accommodates obliquely oriented axons of the rods and cones radiating from the foveal center. These radial fibers, known as the Henle fiber layer, become more prominent in the perifoveal area because of the increasing density of the fibers [15]. At the edge of the foveola, Henle fibers course nearly parallel to the internal limiting membrane. This configuration can yield petaloid or star-shaped patterns on optical imaging when fluid or exudates accumulate within these extracellular spaces. The inner segments of photoreceptors are divided into two distinct regions: the myoid and ellipsoid compartments (Figure 1) [16].

Spectral-domain OCT, with its high resolution of less than 5  $\mu$ m, enables clear observation of retinal microstructures and detailed clinical assessments of the retina [17]. Spectral-domain OCT reveals a pattern of alternating hyperreflective and hyporeflective bands that align with the distinct macular layers identified in histological studies [16, 18]. In spectral-domain OCT images, photoreceptor axons appear as hyporeflective structures and are not readily distinguishable from the adjacent photoreceptor nuclei [14]. Swept-source OCT uses a wavelength-tuning laser and a high-speed detector to capture images quickly, with up to 200 000 A-scans per second, thus reducing motion-related artifacts. Its longer-wavelength light penetrates deeper into eye tissues and provides clearer images through dense media. However, this yields slightly lower axial resolution, typically around 6–8  $\mu$ m [19]. Its effective performance is largely due to the use of a longer wavelength (approximately 1050 nm), which reduces light scattering by the RPE and allows better visualization of deeper eye structures (Figure 2) [20].

## Anatomical Landmarks of the Macula

## Fovea

The macula lutea, a central retinal area approximately 5.5 mm in diameter, is predominantly populated by cone photoreceptors [21]. The fovea centralis, a specialized retinal region approximately 1.5 mm in diameter and located at the center of the macula lutea, contains the highest concentration of cone photoreceptors and is crucial in mediating sharp central vision [22]. High spatial resolution is facilitated by the dense packing of central photoreceptors and the increased proportion of ganglion cells relative to photoreceptors [5].

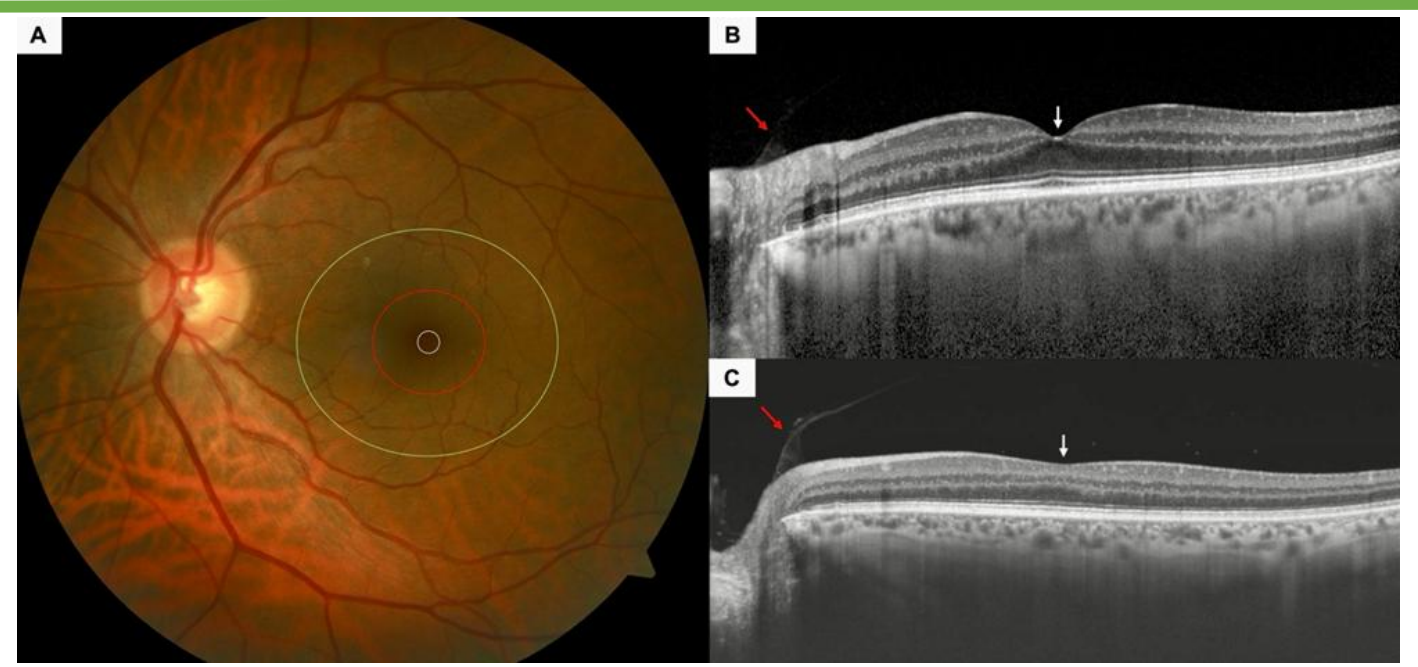


Figure 2. The macula of the left eye in a healthy 59-year-old man. The foveola, fovea, and macula are indicated by white, red, and green circles, respectively, on the color fundus photograph (A). Spectral-domain (Heidelberg Engineering, Heidelberg, Germany) (B) and swept-source (DRI OCT Triton®, Topcon Corporation, Tokyo, Japan) (C) optical coherence tomography images depict the characteristic foveal depression (white arrows) and the distinct stratification of the retinal layers along with peripapillary vitreomacular adhesion (red arrows).

At the center of the fovea, the foveal pit is situated beneath an avascular region and is exclusively populated by cone photoreceptors with elongated outer segments. The foveal pit is bordered by a region in which the inner retinal layers are displaced laterally [23]. During foveal development, cone photoreceptors undergo centripetal migration, axial elongation, and an increase in packing density, all contributing to formation of the foveal pit [24]. One proposed function of the foveal depression is modulation of the retinal refractive properties at the foveal center, as its concave shape optimizes cone photoreceptor compaction and enhances spatial resolution [25]. Roughly half of the primary visual cortex is dedicated to processing inputs originating from the fovea [5]. In the healthy adult retina, the central foveal pit is primarily composed of densely packed cone photoreceptors, whereas the surrounding sloped margins are shaped by the outer plexiform layer and the displaced processes of bipolar cells [22].

The foveal pit potentially compensates for the detrimental effects of chromatic aberration in the eye [26]. The distribution of different cone types in the fovea, such as the concentrations of red and green cones in the foveola, and the highest density of blue cones around the foveola in the lower foveal slope within the avascular zone, may be an adaptation to reduce chromatic aberration in the eye (Figure 3) [5].

Owing to their chemical composition, carotenoids function as optical filters of blue light and offer antioxidant protection by preventing peroxidation of long-chain polyunsaturated fatty acids [27-30]. The filtration of blue light reduces chromatic aberration, thereby improving visual acuity and contrast sensitivity. Additionally, lutein and zeaxanthin alleviate glare discomfort, enhance photostress recovery time, support macular function, and boost neural processing speed [27-30].

The foveal region features an avascular zone, high density of cone photoreceptors, and inward displacement of the inner retinal neurons, all contributing to its unique structural features [24]. The foveal pit apparently achieves optimal optical clarity owing to the lack of blood vessels and inner retinal layers, which helps minimize light scattering [31]. Development of the foveal avascular zone occurs before the foveal pit begins to form [31, 32]. In humans, the diameter of the foveal avascular zone ranges from approximately 0.2 to 1 mm [33]. The avascularization at the foveal center might limit its overall size [34]. No significant correlation has been found between the size of the foveal avascular zone (i.e., the width of the foveal pit) and visual acuity in humans (Figure 4A, B), nor between foveal pit depth and visual acuity in individuals with albinism [5, 35].

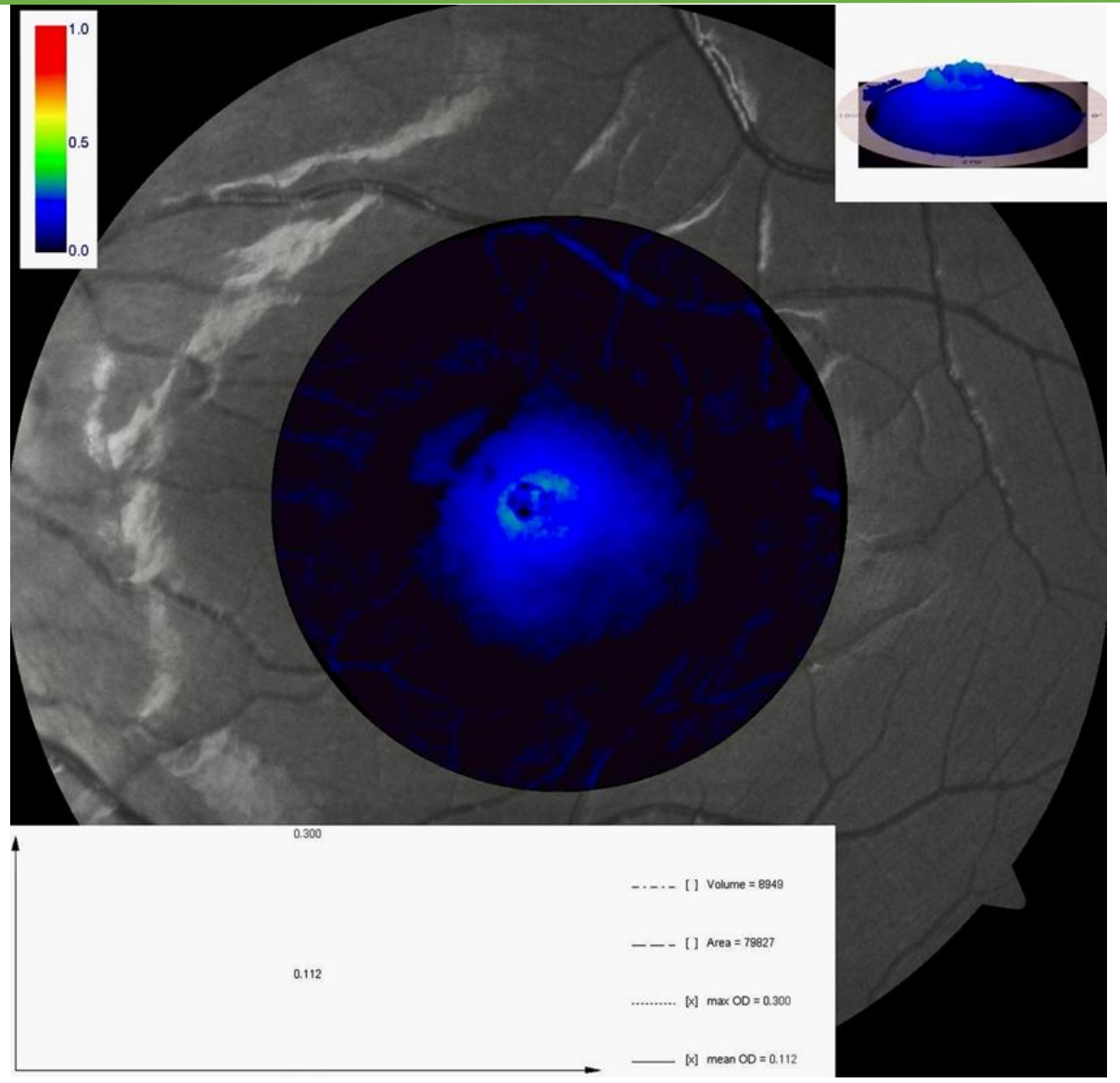


Figure 3. Macular pigment optical density (MPOD) analysis of the left eye of an 8-year-old male patient with no known ocular or systemic abnormalities. The image was obtained using the macular pigment density module of a confocal scanning laser ophthalmoscope (Visucam® 500 digital fundus camera, Carl Zeiss Meditec AG, Jena, Germany). The spatial distribution of macular pigment is visualized, centered on the fovea. The central circular overlay represents MPOD values using a false-color scale, where blue indicates lower density and red indicates higher density, as referenced by the accompanying color bar (range: 0.0–1.0 optical density units [ODU]). Quantitative metrics include a maximum MPOD of 0.300 ODU and a mean MPOD of 0.112 ODU. The estimated macular pigment volume and area are 8949 arbitrary units³ and 79 827 arbitrary units², respectively. The top-right inset provides a 3D surface rendering of pigment density distribution. (Courtesy of Associate Professor Mahmut Kaya.)

The foveal region differs from the other retinal areas in several ways. Its most notable features are the enormously high concentration of neural components and the avascularization within the central fovea (Figure 4C-F). The more subtle distinctions include factors that prevent astrocytes and microglia from populating the area, through mechanisms such as migration or cell death, and the consequences of prolonged exposure to a hypoxic environment during foveal development [2]. Approximately 25% of all retinal ganglion cells are located in the fovea [5].

The fovea has two primary, parallel pathways for processing visual information: one dedicated to high resolution and color discrimination (the midget pathway) and another focused on contrast sensitivity, motion detection, and brightness perception (the diffuse pathway) [36]. Horizontal and amacrine cells transmit information related to contrast, spatial orientation, and movement of visual stimuli. Color differentiation is achieved through two distinct pathways: red-green and blue-yellow [5].

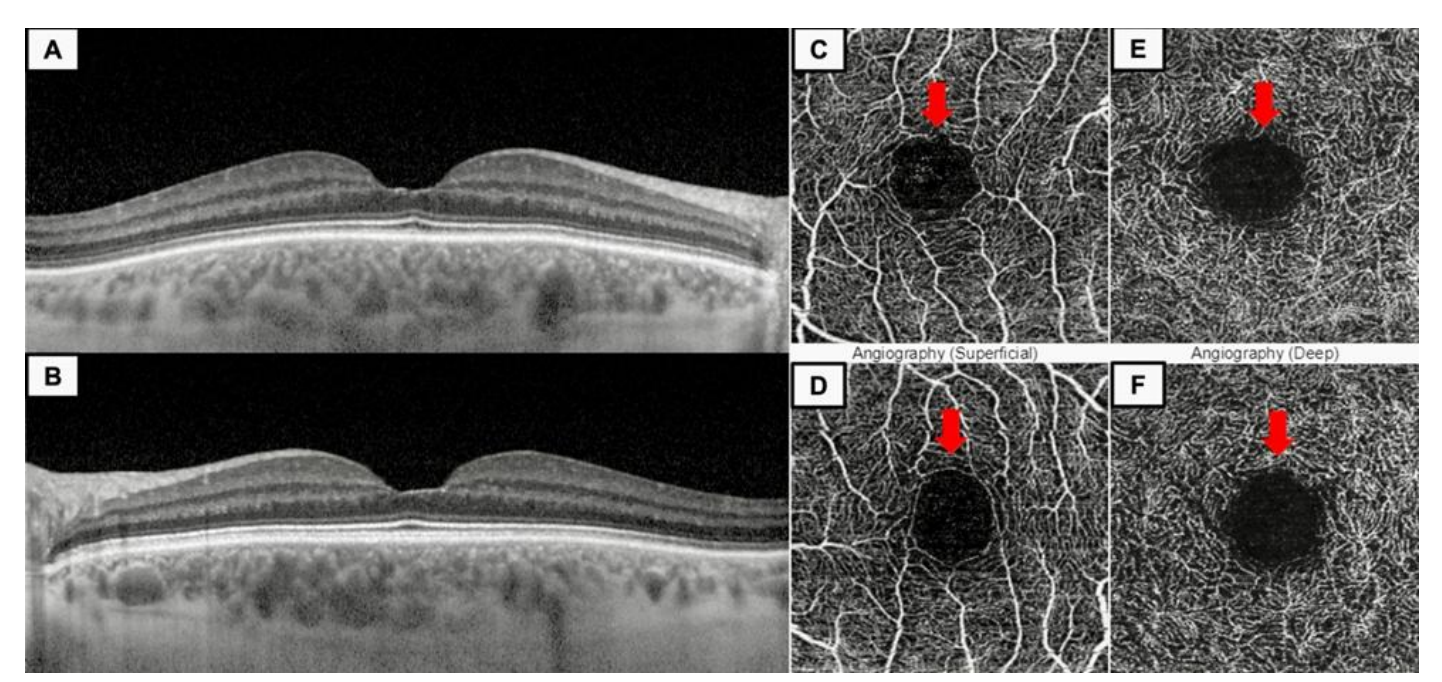


Figure 4. Transfoveal spectral-domain optical coherence tomography (Heidelberg Engineering, Heidelberg, Germany) sections of the right (A) and left (B) eyes of a healthy 56-year-old woman with 20/20 visual acuity demonstrate a slightly enlarged foveal pit in both eyes. Swept-source optical coherence tomography angiography (DRI OCT Triton®, Topcon Corporation, Tokyo, Japan) images of the same patient demonstrate the foveal avascular zone (red arrows) in the superficial (C and D) and deep (E and F) capillary plexuses.

The inner retinal neurons surrounding the foveal center are progressively displaced in a centrifugal direction, whereas the photoreceptor inner segments are centripetally compacted [16]. This intricate remodeling process establishes steep topographical gradients in photoreceptor and ganglion cell densities. Concurrently, the Henle fiber layer exhibits a radiating, star-like configuration, with axonal projections extending outward across the macula from the foveal core [16, 37].

# Henle Fiber Layer

The Henle fiber layer is a specialized component of the outer retina in the macula, primarily consisting of obliquely oriented axons originating from the cone photoreceptors [38]. Its development is closely linked to the maturation of the fovea. As the foveal pit forms, displacement of bipolar cell targets from central cones leads to the characteristic angled orientation of cone axons that defines this layer [5, 38].

The Henle fiber layer exhibits a distinctive radial configuration centered on the fovea, with fibers radiating outward from the foveal center toward the perifovea. This centrifugal pattern extends to a peripheral boundary approximately  $5500 \mu m$  from the fovea [39, 40]. The Henle fiber layer is absent beyond a radial distance of approximately  $8500 \mu m$  from the foveal center [39].

Axons within the Henle fiber layer, like those in other parts of the central nervous system, are elongated tubular structures that contain microtubules. These axons typically measure approximately 558  $\mu$ m in length. The first synapses of these axons occur approximately 350  $\mu$ m from the foveal center, where they synapse with the dendritic processes of bipolar and horizontal cells [37]. A high density of photoreceptor nuclei at the foveal center, combined with their lateral displacement, results in the Henle fiber layer constituting a substantial portion of the macular retinal thickness, as is clearly evident in histological sections [13].

Macular pigment is a yellow xanthophyll substance that is primarily composed of three carotenoid isomers: lutein, zeaxanthin, and meso-zeaxanthin. In the human eye, the highest concentration of macular pigment is found in the Henle fiber layer at the fovea, with a significant reduction in pigment density as distance from the foveal center increases [27, 41].

#### Foveola

The foveola, the innermost part of the fovea, is approximately 350 µm in diameter and a thickness of 90–130 µm. It is within this specific area that visual acuity is at its peak, reaching 100% [42, 43]. However, the foveolar dimensions showed considerable inter-individual variability. Some individuals have a small yet thick foveola characterized by a centrally thickened outer nuclear layer, and remnants of the inner retinal layers may persist within the central fovea. In some individuals, the foveola appears broad, flat, and thin, with the outer nuclear layer forming a V-shaped profile and reaching its greatest thickness toward the edges rather than the center [23].

The foveola is composed of four layers located in front of the fovea externa: the inner layer, Henle fiber layer, outer nuclear layer, and layer containing the processes of the outer cone cells. The inner layer of the foveola that fills the bottom of the foveal pit is primarily composed of Muller cell bodies and their processes [44].

The foveola is devoid of rods, ganglion cells, inner nuclear layer neurons, and short-wavelength-sensitive cone photoreceptors (S-cones), resulting in a region primarily composed of cone photoreceptor cell bodies. However, a few parasol (P-) ganglion cells may be present, forming part of the innermost cell layer [2, 45]. At the very center of the foveal cone mosaic lies a tiny area, approximately 0.1 millimeters wide, and lacks S-cones. Consequently, fine visual details in this region are processed mainly by long- and medium-wavelength cones (L- and M-cones) [45].

Cone photoreceptors and Muller glial cells are responsible for the structural formation of the foveolar [5]. In the human retina, the foveola comprises approximately 25–35 uniquely specialized Muller glial cells. These Muller cells are considered atypical, because their cellular processes remain confined within the boundaries of the foveola [44]. Specialized Muller cells in the foveola only connect with the central cone photoreceptors and do not interact with synapses or other neurons. Unlike typical Muller cells, they do not form a functional column between the photoreceptors and neurons [5]. The processes of the Muller cells that course along the inner surface of the foveola are typically extremely thin, with a thickness comparable to that of the basal lamina of the internal limiting membrane's basal lamina [46]. The basal lamina of the internal limiting membrane exhibits morphological differences between the foveal and its walls. In the foveola, the basal lamina is a thin extracellular matrix sheet, whereas it is considerably thicker in the foveal and parafoveal walls, it is considerably thicker [47].

The unique Muller cells located within the foveola are believed to serve multiple functions. They exhibit a high concentration of macular pigments, and because of the specific arrangement of the cone photoreceptors in this region, the central foveola shows a pronounced peak in macular pigment density [5].

Within the foveola, oxygen diffuses approximately  $100~\mu m$  from the choriocapillaris to reach the inner segments of cone photoreceptors, as this region lacks a supplementary supply from retinal vasculature. In contrast, in other retinal regions, the diffusion distance from the choriocapillaris to the photoreceptor inner segments is shorter, averaging 50 to  $60~\mu m$  [2].

## Parafovea

The macula is anatomically divided into the fovea (approximately 1.5 mm) and the surrounding parafovea (approximately 2.3 mm), each with a distinct cellular composition [21]. Encircling the fovea, the parafoveal region is distinguished by a sparse vascular network, exceptionally high concentration of ganglion cells, and relatively low rod density. Consequently, the local rod-to-cone ratio was approximately 4:1, which was markedly lower than that in the perifoveal region, where the ratio ranged from 33:1 to 130:1 [2].

The parafoveal region of the human macula has distinct anatomical and physiological features, including a densely packed cellular architecture and elevated metabolic activity. Within this zone, the Henle fiber layer extends obliquely through the area traditionally identified as the outer nuclear layer on OCT [4, 48]. The outer plexiform layer, which was loosely structured in this region, functioned as a potential space for fluid accumulation. Moreover, the limited fluid clearance capacity attributable to the absence of retinal vasculature in the foveal avascular zone contributes to this predisposition. Consequently, the parafovea is particularly vulnerable to the initial appearance of extravascular fluid [49, 50].

#### Perifovea

The outermost anatomical region of the macula, known as the perifovea, functions as a transition zone between the highly specialized central retina and the more generalized peripheral retina. It is characterized by a dense network of retinal blood vessels and an increasing ratio of rod-to-cone photoreceptors, features resembling those of the peripheral

retina [51].

# Clinical and Surgical Relevance to the Macular Anatomy

Muller cells are the sole macroglial cell types present in the central region of the fovea [5]. In the foveola, photoreceptor cells are encased by outward extensions of typical Muller cells originating from the foveal walls. The structural formation of the fovea involves outward (centrifugal) migration of the inner retinal layers and inward (centripetal) movement of the outer retinal components [37]. The thin inner extensions of Muller cells, which run beneath and along the basal lamina of the foveola, form a network that likely helps protect the tissue by resisting stretching forces from different directions [44]. Mechanical traction affecting the central fovea can arise in conditions such as cystoid macular edema or partial posterior vitreous detachment [52].

In cystoid macular edema, fluid-filled cystic spaces may develop within the foveola, leading to separation of the inner layer of Muller cells [5, 52]. Despite detachment, the Muller cell layer often maintains structural cohesion between the foveal walls. Damage to the Muller cell layer within the foveola is a key event contributing to the development of a macular hole [5]. It has been proposed that the mechanical tension generated by Muller cells in the fovea contributes to the reestablishment of normal foveal architecture following macular hole repair surgery [53]. This pathophysiological process has been visualized using OCT and is characterized by the presence of intraretinal hyperreflective lines. This relatively novel and distinctive OCT feature is thought to arise from various forms of damage to Muller cells at the fovea [54, 55]. Although intraretinal hyperreflective lines have been documented in a variety of retinal pathologies, they are most frequently observed during the postoperative healing phase following vitreoretinal surgery for full-thickness macular holes, in the pre-hole stage, or in association with lamellar macular holes [54, 55]. These findings suggest that Muller cell activity plays a central role in both the pathogenesis and reparative processes of these conditions. The ability to visualize this phenomenon using OCT is likely attributed to the distinct anatomical and histological features of foveal Muller cells, which differ markedly from those in other regions of the retina [54, 55].

The Henle fiber layer consists of Muller cells and photoreceptor axons, which extend radially toward the outer plexiform layer. Distortion of the Henle fiber layer leads to characteristic findings on cross-sectional OCT imaging, such as a hyperreflective Henle fiber layer over the drusen [13]. Because of the different reflectance properties of the Henle fiber layer, the OCT appearances of the outer plexiform layer/Henle fiber layer interface have been previously categorized as bright, columnar, dentate, delimited, indistinct, or dark [9]. The unique structure of the Henle fiber layer has significant pathophysiological implications. It plays a role in the formation of a macular star in exudative and inflammatory retinopathies, development of radially oriented cystoid macular edema, and radial or petaloid hemorrhages within the Henle fiber layer. These changes can occur in both local conditions, such as branch and central retinal vein occlusion, and in systemic venous disorders, such as intracranial hemorrhage. They are associated with macular telangiectasia type 2 [27]. In tractional retinopathies, these fibers may become distended and separate the outer nuclear layer from the rest of the outer plexiform layer [15, 56].

Additionally, in certain macular diseases, such as acute macular neuroretinopathy and acute posterior multifocal placoid pigment epitheliopathy, a distinctive hyperreflective lesion mirroring the angulation of the Henle fiber layer and extending further from the outer plexiform layer to the ellipsoid/inner segment has been reported on OCT (angular sign of Henle fiber layer hyperreflectivity) [27].

This review provides a clinically relevant and anatomically detailed overview of the macula and highlights the interplay between structural organization and retinal imaging. One of its key strengths is its translational value, which offers insights that are directly applicable in both diagnostic and therapeutic contexts. However, the narrative format limits systematic comparisons across the full breadth of available evidence. Moreover, this review did not explore longitudinal or population-based variations in the macular architecture. Future research should aim to translate anatomical insights into tools for the early diagnosis and personalized management of macular diseases, while also investigating how emerging imaging technologies can address current diagnostic limitations.

## **CONCLUSIONS**

The macula is a masterpiece of the retinal architecture, with the fovea at its center driving sharp, color-sensitive vision. From the unique cone-packed foveola to the radially oriented Henle fiber layer, each structure plays a vital role in maintaining visual precision. Understanding these intricate layers and their interplay with the surrounding cells is

crucial for diagnosing and treating macular disorders. Ultimately, a deep understanding of the macular anatomy is crucial for preserving visual function and improving treatment outcomes. This review provides a practical anatomical resource for clinicians and researchers engaged in diagnosis and treatment of macular entities. Further research is needed to investigate how advanced imaging technologies may improve the early diagnosis and management of macular diseases.

## **ETHICAL DECLARATIONS**

**Ethical approval:** This narrative review received ethical approval at the departmental level of the Faculty of Medicine, Dokuz Eylul University, Izmir, Turkey. All figures presented were obtained from the patient documentation archives of our unit and informed consent was obtained from each patient before inclusion in the review.

Conflict of interest: None.

## **FUNDING**

None.

#### **ACKNOWLEDGMENTS**

None.

## **REFERENCES**

- Kirby ML, Galea M, Loane E, Stack J, Beatty S, Nolan JM. Foveal anatomic associations with the secondary peak and the slope of the macular pigment spatial profile. Invest Ophthalmol Vis Sci. 2009 Mar;50(3):1383-91. doi: 10.1167/iovs.08-2494. Epub 2008 Oct 20. PMID: 18936143.
- Provis JM, Penfold PL, Cornish EE, Sandercoe TM, Madigan MC. Anatomy and development of the macula: specialisation and the vulnerability to macular degeneration. Clin Exp Optom. 2005 Sep;88(5):269-81. doi: 10.1111/j.1444-0938.2005.tb06711.x. PMID: 16255686.
- 3. Rehman I, Mahabadi N, Motlagh M, Ali T. Anatomy, Head and Neck, Eye Fovea. 2023 Aug 28. In: StatPearls [Internet]. Treasure Island (FL): StatPearls Publishing; 2025 Jan–. PMID: 29493926.
- Bringmann A, Barth T, Ziemssen F. Morphology of foveal hypoplasia: Hyporeflective zones in the Henle fiber layer of eyes with high-grade foveal hypoplasia. PLoS One. 2022 Apr 13;17(4):e0266968. doi: 10.1371/journal.pone.0266968. PMID: 35417487; PMCID: PMC9007365.
- 5. Bringmann A, Syrbe S, Görner K, Kacza J, Francke M, Wiedemann P, Reichenbach A. The primate fovea: Structure, function and development. Prog Retin Eye Res. 2018 Sep;66:49-84. doi: 10.1016/j.preteyeres.2018.03.006. Epub 2018 Mar 30. PMID: 29609042.
- Gupta MP, Herzlich AA, Sauer T, Chan CC. Retinal Anatomy and Pathology. Dev Ophthalmol. 2016;55:7-17. doi: 10.1159/000431128. Epub 2015 Oct 26. PMID: 26502225.
- Jackson GR, Owsley C, Curcio CA. Photoreceptor degeneration and dysfunction in aging and age-related maculopathy. Ageing Res Rev. 2002 Jun;1(3):381-96. doi: 10.1016/s1568-1637(02)00007-7. PMID: 12067593.
- 8. Mahabadi N, Al Khalili Y. Neuroanatomy, Retina. 2023 Aug 8. In: StatPearls [Internet]. Treasure Island (FL): StatPearls Publishing; 2025 Jan–. PMID: 31424894.
- Ouyang Y, Walsh AC, Keane PA, Heussen FM, Pappuru RK, Sadda SR. Different phenotypes of the appearance of the outer plexiform layer on optical coherence tomography. Graefes Arch Clin Exp Ophthalmol. 2013 Oct;251(10):2311-7. doi: 10.1007/s00417-013-2308-5. Epub 2013 May 10. PMID: 23661097.
- Staurenghi G, Sadda S, Chakravarthy U, Spaide RF; International Nomenclature for Optical Coherence Tomography (IN OCT)
  Panel. Proposed lexicon for anatomic landmarks in normal posterior segment spectral-domain optical coherence tomography:
  the IN OCT consensus. Ophthalmology. 2014 Aug;121(8):1572-8. doi: 10.1016/j.ophtha.2014.02.023. Epub 2014 Apr 19. PMID: 24755005
- 11. Ershov AV, Bazan NG. Photoreceptor phagocytosis selectively activates PPARgamma expression in retinal pigment epithelial cells. J Neurosci Res. 2000 May 1;60(3):328-37. doi: 10.1002/(SICI)1097-4547(20000501)60:3<328::AID-JNR7>3.0.CO;2-5. PMID: 10797535.
- 12. Handa JT. How does the macula protect itself from oxidative stress? Mol Aspects Med. 2012 Aug;33(4):418-35. doi: 10.1016/j.mam.2012.03.006. Epub 2012 Apr 5. PMID: 22503691; PMCID: PMC3392444.
- Lujan BJ, Roorda A, Knighton RW, Carroll J. Revealing Henle's fiber layer using spectral domain optical coherence tomography. Invest Ophthalmol Vis Sci. 2011 Mar 18;52(3):1486-92. doi: 10.1167/iovs.10-5946. PMID: 21071737; PMCID: PMC3101665.
- Vajzovic L, Hendrickson AE, O'Connell RV, Clark LA, Tran-Viet D, Possin D, Chiu SJ, Farsiu S, Toth CA. Maturation of the human fovea: correlation of spectral-domain optical coherence tomography findings with histology. Am J Ophthalmol. 2012 Nov;154(5):779-789.e2. doi: 10.1016/j.ajo.2012.05.004. Epub 2012 Aug 13. PMID: 22898189; PMCID: PMC3612897.
- 15. Griffin SM, McDonald HR, Johnson RN, Jumper JM, Fu AD, Cunningham ET Jr, Kiang L, Ng CC, Lujan BJ. FINGERPRINT SIGN OF THE HENLE FIBER LAYER. Retina. 2021 Feb 1;41(2):381-386. doi: 10.1097/IAE.00000000000002875. PMID: 32604343; PMCID: PMC7959252.

- Curcio CA, Messinger JD, Sloan KR, Mitra A, McGwin G, Spaide RF. Human chorioretinal layer thicknesses measured in macula-wide, high-resolution histologic sections. Invest Ophthalmol Vis Sci. 2011 Jun 6;52(7):3943-54. doi: 10.1167/iovs.10-6377. PMID: 21421869; PMCID: PMC3175964.
- 17. Drexler W, Morgner U, Ghanta RK, Kärtner FX, Schuman JS, Fujimoto JG. Ultrahigh-resolution ophthalmic optical coherence tomography. Nat Med. 2001 Apr;7(4):502-7. doi: 10.1038/86589. Erratum in: Nat Med 2001 May;7(5):636. PMID: 11283681; PMCID: PMC1950821.
- Anger EM, Unterhuber A, Hermann B, Sattmann H, Schubert C, Morgan JE, Cowey A, Ahnelt PK, Drexler W. Ultrahigh resolution optical coherence tomography of the monkey fovea. Identification of retinal sublayers by correlation with semithin histology sections. Exp Eye Res. 2004 Jun;78(6):1117-25. doi: 10.1016/j.exer.2004.01.011. PMID: 15109918.
- Li Y, Zheng F, Foo LL, Wong QY, Ting D, Hoang QV, Chong R, Ang M, Wong CW. Advances in OCT Imaging in Myopia and Pathologic Myopia. Diagnostics (Basel). 2022 Jun 8;12(6):1418. doi: 10.3390/diagnostics12061418. PMID: 35741230; PMCID: PMC9221645.
- Monferrer-Adsuara C, Remolí-Sargues L, Navarro-Palop C, Cervera-Taulet E, Montero-Hernández J, Medina-Bessó P, Castro-Navarro V. Swept-source optical coherence tomography early findings in patients with carotid artery disease. Eur J Ophthalmol. 2025 Jan;35(1):324-334. doi: 10.1177/11206721241265388. Epub 2024 Jul 26. PMID: 39056140.
- 21. Tschulakow AV, Oltrup T, Bende T, Schmelzle S, Schraermeyer U. The anatomy of the foveola reinvestigated. PeerJ. 2018 Mar 12;6:e4482. doi: 10.7717/peerj.4482. PMID: 29576957; PMCID: PMC5853608.
- Singh SR, Vaidya H, Borrelli E, Chhablani J. Foveal photoreceptor disruption in ocular diseases: An optical coherence tomography-based differential diagnosis. Surv Ophthalmol. 2023 Jul-Aug;68(4):655-668. doi: 10.1016/j.survophthal.2023.03.003. Epub 2023 Mar 18. PMID: 36934831.
- 23. Tick S, Rossant F, Ghorbel I, Gaudric A, Sahel JA, Chaumet-Riffaud P, Paques M. Foveal shape and structure in a normal population. Invest Ophthalmol Vis Sci. 2011 Jul 29;52(8):5105-10. doi: 10.1167/jovs.10-7005. PMID: 21803966.
- Dubis AM, Costakos DM, Subramaniam CD, Godara P, Wirostko WJ, Carroll J, Provis JM. Evaluation of normal human foveal development using optical coherence tomography and histologic examination. Arch Ophthalmol. 2012 Oct;130(10):1291-300. doi: 10.1001/archophthalmol.2012.2270. PMID: 23044942; PMCID: PMC3724218.
- 25. Zouache MA, Silvestri G, Amoaku WM, Silvestri V, Hubbard WC, Pappas C, Akafo S, Lartey S, Mastey RR, Carroll J, Hageman GS. Comparison of the Morphology of the Foveal Pit Between African and Caucasian Populations. Transl Vis Sci Technol. 2020 Apr 28;9(5):24. doi: 10.1167/tvst.9.5.24. PMID: 32821496; PMCID: PMC7401974.
- Marmor MF, Choi SS, Zawadzki RJ, Werner JS. Visual insignificance of the foveal pit: reassessment of foveal hypoplasia as fovea plana. Arch Ophthalmol. 2008 Jul;126(7):907-13. doi: 10.1001/archopht.126.7.907. PMID: 18625935; PMCID: PMC2584610.
- Ramtohul P, Cabral D, Sadda S, Freund KB, Sarraf D. The OCT angular sign of Henle fiber layer (HFL) hyperreflectivity (ASHH) and the pathoanatomy of the HFL in macular disease. Prog Retin Eye Res. 2023 Jul;95:101135. doi: 10.1016/j.preteyeres.2022.101135. Epub 2022 Nov 1. PMID: 36333227.
- 28. Stringham JM, Hammond BR Jr. The glare hypothesis of macular pigment function. Optom Vis Sci. 2007 Sep;84(9):859-64. doi: 10.1097/OPX.0b013e3181559c2b. PMID: 17873771.
- Nolan JM, Loughman J, Akkali MC, Stack J, Scanlon G, Davison P, Beatty S. The impact of macular pigment augmentation on visual performance in normal subjects: COMPASS. Vision Res. 2011 Mar 2;51(5):459-69. doi: 10.1016/j.visres.2010.12.016. Epub 2011 Jan 13. PMID: 21237188.
- Hammond BR, Fletcher LM, Roos F, Wittwer J, Schalch W. A double-blind, placebo-controlled study on the effects of lutein and zeaxanthin on photostress recovery, glare disability, and chromatic contrast. Invest Ophthalmol Vis Sci. 2014 Dec 2;55(12):8583-9. doi: 10.1167/iovs.14-15573. PMID: 25468896.
- 31. Chui TY, Zhong Z, Song H, Burns SA. Foveal avascular zone and its relationship to foveal pit shape. Optom Vis Sci. 2012 May;89(5):602-10. doi: 10.1097/OPX.0b013e3182504227. PMID: 22426172; PMCID: PMC3348263.
- 32. Provis JM, Sandercoe T, Hendrickson AE. Astrocytes and blood vessels define the foveal rim during primate retinal development. Invest Ophthalmol Vis Sci. 2000 Sep;41(10):2827-36. PMID: 10967034.
- 33. Dubis AM, Hansen BR, Cooper RF, Beringer J, Dubra A, Carroll J. Relationship between the foveal avascular zone and foveal pit morphology. Invest Ophthalmol Vis Sci. 2012 Mar 21;53(3):1628-36. doi: 10.1167/iovs.11-8488. PMID: 22323466; PMCID: PMC3339921.
- 34. Franco EC, Finlay BL, Silveira LC, Yamada ES, Crowley JC. Conservation of absolute foveal area in New World monkeys. A constraint on eye size and conformation. Brain Behav Evol. 2000 Nov;56(5):276-86. doi: 10.1159/000047211. PMID: 11251320.
- Mohammad S, Gottlob I, Kumar A, Thomas M, Degg C, Sheth V, Proudlock FA. The functional significance of foveal abnormalities in albinism measured using spectral-domain optical coherence tomography. Ophthalmology. 2011 Aug;118(8):1645-52. doi: 10.1016/j.ophtha.2011.01.037. Epub 2011 May 12. PMID: 21570122.
- Masri RA, Grünert U, Martin PR. Analysis of Parvocellular and Magnocellular Visual Pathways in Human Retina. J Neurosci. 2020 Oct 14;40(42):8132-8148. doi: 10.1523/JNEUROSCI.1671-20.2020. Epub 2020 Oct 2. PMID: 33009001; PMCID: PMC7574660.
- 37. Drasdo N, Millican CL, Katholi CR, Curcio CA. The length of Henle fibers in the human retina and a model of ganglion receptive field density in the visual field. Vision Res. 2007 Oct;47(22):2901-11. doi: 10.1016/j.visres.2007.01.007. Epub 2007 Feb 22. PMID: 17320143; PMCID: PMC2077907.
- 38. Habibi A, Ashrafkhorasani M, Santina A, Emamverdi M, Corradeti G, Abbasgholizadeh R, Nittala MG, Freund KB, Sarraf D, Sadda SR. Evaluating fingerprint-like patterns in the healthy Henle fiber layer using enface OCT imaging. Exp Eye Res. 2024 Aug;245:109979. doi: 10.1016/j.exer.2024.109979. Epub 2024 Jun 22. PMID: 38909669.
- Quinn N, Csincsik L, Flynn E, Curcio CA, Kiss S, Sadda SR, Hogg R, Peto T, Lengyel I. The clinical relevance of visualising the peripheral retina. Prog Retin Eye Res. 2019 Jan;68:83-109. doi: 10.1016/j.preteyeres.2018.10.001. Epub 2018 Oct 10. PMID: 30316018.
- Mrejen S, Gallego-Pinazo R, Freund KB, Paques M. Recognition of Henle's fiber layer on OCT images. Ophthalmology. 2013 Jun;120(6):e32-3.e1. doi: 10.1016/j.ophtha.2013.01.039. PMID: 23732066.

- 41. Trieschmann M, van Kuijk FJ, Alexander R, Hermans P, Luthert P, Bird AC, Pauleikhoff D. Macular pigment in the human retina: histological evaluation of localization and distribution. Eye (Lond). 2008 Jan;22(1):132-7. doi: 10.1038/sj.eye.6702780. Epub 2007 Mar 30. PMID: 17401321.
- 42. Trauzettel-Klosinski S. Rehabilitation for visual disorders. J Neuroophthalmol. 2010 Mar;30(1):73-84. doi: 10.1097/WNO.0b013e3181ce7e8f. PMID: 20182214.
- 43. Yanni SE, Wang J, Chan M, Carroll J, Farsiu S, Leffler JN, Spencer R, Birch EE. Foveal avascular zone and foveal pit formation after preterm birth. Br J Ophthalmol. 2012 Jul;96(7):961-6. doi: 10.1136/bjophthalmol-2012-301612. Epub 2012 Apr 29. PMID: 22544530.
- 44. Syrbe S, Kuhrt H, Gärtner U, Habermann G, Wiedemann P, Bringmann A, Reichenbach A. Müller glial cells of the primate foveola: An electron microscopical study. Exp Eye Res. 2018 Feb;167:110-117. doi: 10.1016/j.exer.2017.12.004. Epub 2017 Dec 11. PMID: 29242027.
- 45. Kreis J, Carroll J. Applications of Adaptive Optics Imaging for Studying Conditions Affecting the Fovea. Annu Rev Vis Sci. 2024 Sep;10(1):239-262. doi: 10.1146/annurev-vision-102122-100022. Epub 2024 Sep 2. PMID: 38635871.
- 46. Ponsioen TL, van Luyn MJ, van der Worp RJ, Pas HH, Hooymans JM, Los LI. Human retinal Müller cells synthesize collagens of the vitreous and vitreoretinal interface in vitro. Mol Vis. 2008 Mar 26;14:652-60. PMID: 18385800; PMCID: PMC2276182.
- 47. Henrich PB, Monnier CA, Halfter W, Haritoglou C, Strauss RW, Lim RY, Loparic M. Nanoscale topographic and biomechanical studies of the human internal limiting membrane. Invest Ophthalmol Vis Sci. 2012 Jun 29;53(6):2561-70. doi: 10.1167/iovs.11-8502. PMID: 22410559.
- 48. Ni S, Khan S, Nguyen TP, Ng R, Lujan BJ, Tan O, Huang D, Jian Y. Volumetric directional optical coherence tomography. Biomed Opt Express. 2022 Jan 21;13(2):950-961. doi: 10.1364/BOE.447882. PMID: 35284155; PMCID: PMC8884206.
- 49. Scholl S, Kirchhof J, Augustin AJ. Pathophysiology of macular edema. Ophthalmologica. 2010;224 Suppl 1:8-15. doi: 10.1159/000315155. Epub 2010 Aug 18. PMID: 20714176.
- Brynskov T, Laugesen CS, Floyd AK, Sørensen TL. Thickening of inner retinal layers in the parafovea after bariatric surgery in patients with type 2 diabetes. Acta Ophthalmol. 2016 Nov;94(7):668-674. doi: 10.1111/aos.13087. Epub 2016 May 26. PMID: 27226121.
- 51. Chan G, Balaratnasingam C, Yu PK, Morgan WH, McAllister IL, Cringle SJ, Yu DY. Quantitative morphometry of perifoveal capillary networks in the human retina. Invest Ophthalmol Vis Sci. 2012 Aug 13;53(9):5502-14. doi: 10.1167/iovs.12-10265. PMID: 22815351.
- 52. Johnson MW. Perifoveal vitreous detachment and its macular complications. Trans Am Ophthalmol Soc. 2005;103:537-67. PMID: 17057817; PMCID: PMC1447588.
- 53. Chung H, Byeon SH. New insights into the pathoanatomy of macular holes based on features of optical coherence tomography. Surv Ophthalmol. 2017 Jul-Aug;62(4):506-521. doi: 10.1016/j.survophthal.2017.03.003. Epub 2017 Mar 11. PMID: 28300548.
- Kayabasi M, Koksaldi S, Saatci AO. Intraretinal hyperreflective line: potential biomarker in various retinal disorders. Med Hypothesis Discov Innov Ophthalmol. 2024 Oct 14;13(3):129-138. doi: 10.51329/mehdiophthal1504. PMID: 39507809; PMCID: PMC11537236.
- 55. Scharf JM, Hilely A, Preti RC, Grondin C, Chehaibou I, Greaves G, Tran K, Wang D, Ip MS, Hubschman JP, Gaudric A, Sarraf D. Hyperreflective Stress Lines and Macular Holes. Invest Ophthalmol Vis Sci. 2020 Apr 9;61(4):50. doi: 10.1167/iovs.61.4.50. PMID: 32347919; PMCID: PMC7401923.
- 56. Govetto A, Hubschman JP, Sarraf D, Figueroa MS, Bottoni F, dell'Omo R, Curcio CA, Seidenari P, Delledonne G, Gunzenhauser R, Ferrara M, Au A, Virgili G, Scialdone A, Repetto R, Romano MR. The role of Müller cells in tractional macular disorders: an optical coherence tomography study and physical model of mechanical force transmission. Br J Ophthalmol. 2020 Apr;104(4):466-472. doi: 10.1136/bjophthalmol-2019-314245. Epub 2019 Jul 20. PMID: 31326893.